ACI MATERIALS JOURNAL TECHNICAL PAPER

Title no. 105-M20

# Nanoscale Characterization of Cementitious Materials

by Paramita Mondal, Surendra P. Shah, and Laurence D. Marks

*It is widely believed that the fundamental properties of concrete are affected by the material properties at the nanoscale. Hence, to improve cement and concrete properties, it is necessary to first understand the nanoscale properties. In this research, sample preparation techniques were developed to image the nano- and microstructure of hardened cement paste using atomic force microscopy (AFM). A special type of nanoindenter along with in-place scanning probe microscopy imaging has been used to determine the nanoscale local mechanical properties, including the Young's modulus of the interfacial transition zone.*

**Keywords:** atomic force microscopy; cement paste nanostructure; interfacial transition zone; mechanical properties; nanoindentation.

## INTRODUCTION

Concrete is heterogeneous at all length scale with very complex micro- and nano-structure. To be able to control macroscopic properties and develop new nano-engineered materials, it is necessary to study the cement paste nano-structure and understand how this relates to the local mechanical properties.

Atomic force microscopy (AFM)[1] with a local probe can in principle determine local mechanical properties along with high-resolution imaging, and it is just starting to be used to study the nanostructure of cementitious materials.[2-8] For example, AFM has been used to study the surface changes of cement clinker immersed initially in saturated calcium hydroxide solution, followed by water and sucrose solution;[2] the change in hydrated cement paste microstructure with exposure to different humidity levels;[3] the carbonation process of calcium hydroxide present in hydrated cement paste;[4] and for imaging the denser microstructure of the cement paste with silica fume or fly ash.[5] One advantage of AFM is that it can be used with a special diamond indenter probe to extract nanoscale local mechanical properties along with high-resolution imaging. This has been successfully implemented for different soft materials[9]; but, in general, it only provides qualitative information and proportional values for the elastic modulus.[10,11] A different type of local probe—nanoindentation—has proved to be a reliable technique to quantitatively determine local mechanical properties.[12-18] The disadvantage of nanoindentation is the absence of any imaging ability, which is an issue for heterogeneous materials such as cement paste. To overcome this problem, in some recent nanoindentation studies, a large number of indentations were performed on hydrated cement paste samples and the calculated modulus values were grouped statistically to obtain the modulus of different phases present.[16,17] In another study, to make the experiment more reliable, a cold field emission scanning electron microscope (CFE-SEM) was used to add an imaging capability.[13]

In this paper, results from an extensive atomic force microscopy study of the nanostructure of cement paste are presented. A special type of nanoindenter, triboindenter was used that combines nanoindentation to determine the local mechanical properties at the nanoscale with high-resolution in-place scanning probe microscopy (SPM) imaging that allows pre- and post-test observation of the sample. A triboindenter allows for a more direct approach where one can identify different phases in cement paste through imaging and determine the local mechanical properties of these phases with minimal ambiguity. This unique advantage has already been used in the case of other materials.[19] This paper presents results of nano-mechanical testing on cement paste and on mortar samples. The imaging technique along with nanoindentation proved to be the most advantageous in determining the local mechanical properties of the interfacial transition zone.

As studied by many researchers, the interfacial transition zone (ITZ) is the region of cement paste around aggregate particles that develops due to the so-called wall effect of cement particles packing against a much larger, relatively smooth aggregate surface.[20] This is a region of gradual transition where the effective thickness varies with the microstructural feature being studied and the degree of hydration.[21] In many studies, it was concluded that in ordinary portland cement concrete, the ITZ consists of a region up to 50 μm around each aggregate with less unhydrated particles, less calcium-silicate-hydrate, higher porosity, and greater concentration of calcium hydroxide and ettringite. Simeonov and Ahmad[22] reported the influence of ITZ on the overall elastic properties of mortar and concrete. In normal concrete, it is considered to be the weakest link in the mechanical system.[21,23] Although it is widely accepted that the properties of the ITZ have to be taken into account in modeling the overall mechanical properties of concrete,[20,22-28] it is difficult to determine its local mechanical properties because of the complexity of the structure and the constrains of existing measurement techniques.[29] Most of the time, the modulus of ITZ is assumed to be uniform and less than that of the paste matrix by a constant factor.[24] This factor is assumed to have a value between 0.2 and 0.8, although there is no theory or experimental data to support this assumption.[28] In their model, Lutz et al.[26] assumed that the elastic properties vary smoothly as a power law within the ITZ. By fitting macroscopic bulk modulus data, they found that the modulus of ITZ is 30 to 50% less than that of the bulk matrix. In some recent studies, attempts were made to determine the local mechanical properties of the ITZ using microindentation or microhardness testing,[30-32] but there is little information available at the nanoscale.

*ACI Materials Journal*, V. 105, No. 2, March-April 2008.
MS No. M-2007-010.R1 received March 6, 2007, and reviewed under Institute publication policies.  Pertinent discussion including authors' closure, if any, will be published in the January-February 2009 *ACI Materials Journal* if the discussion is received by October 1, 2008.

**Paramita Mondal** *is a PhD Candidate in the Department of Civil and Environmental Engineering at Northwestern University, Evanston, IL. She received her master's degree from the University of Connecticut, Storrs, CT, in 2004 and her bachelor's degree from Jadavpur University, India, in 2001. Her research interests include nano- and micro-scale characterization of cementitious materials, nano- to macro-scale modeling, and use of nanotechnology to improve properties and performance of concrete.*

**Surendra P. Shah**, *FACI, is a Walter P. Murphy Professor of Civil Engineering at Northwestern University and the Director of the Center for Advanced Cement-Based Materials. He received the ACI Anderson Award and Robert Philleo Award. He is a member of ACI Committees 363, High-Strength Concrete; 440, Fiber Reinforced Polymer Reinforcement; 446, Fracture Mechanics; 548, Polymers in Concrete; and 549, Thin Reinforced Cementitious Products and Ferrocement. He is the past Chair of Committees 215, Fatigue of Concrete, and 544, Fiber-Reinforced Concrete. His research interests include connecting microscopic behavior to structural response of concrete, constitutive relationships, nondestructive testing, failure of concrete, durability, fiber-reinforced concrete, and self-consolidating concrete.*

**Laurence D. Marks** *is a Professor of Materials Science and Engineering at Northwestern University. His research interests include transmission electron microscopy, in-place experiments, microscopy of surfaces, surface structure, tribology, and cement nanostructure and nanoscale mechanical properties.*

## RESEARCH SIGNIFICANCE

This is an interdisciplinary research with a goal to improve the understanding of the basic properties of concrete and cementitious materials. This research provides a better understanding of the nanostructure of cement paste and nanoscale local mechanical properties. This also provides better insight into the mechanical properties of ITZ. Findings from this research will provide better input for modeling the nanoscale properties of cementitious materials.

## SAMPLE PREPARATION

Sample preparation is a very important step because it affects the microstructure. Getting an extremely smooth surface is critical for AFM because the ability to image the intrinsic micro- and nano-structure of a sample depends on effective elimination of the sample roughness without any damage. Having a smooth surface is also necessary for the determination of reliable local mechanical properties. Cubes of cement paste 1 x 1 x 1 in. (25.4 x 25.4 x 25.4 mm) were made out of Type I portland cement with a water-cement ratio (*w/cm*) of 0.5. Samples were demolded after 24 hours, and then cured at 77 °F (25 °C) under water for 6 months. Once cured, approximately 1/5 in. (5 mm) thin sections were cut out of these specimens and mounted on a metal sample holder using an adhesive (softening temperature: 159.8 °F [71° C]) for polishing. Different polishing techniques were studied to understand the effectiveness of these techniques and estimate the damaging effect that might be associated with them.

Samples were successively dry polished using paper discs of gradation 34.2 μm, 22.1 μm, 14.5 μm, and 6.5 μm. The use of water was avoided at these steps to prevent any damage. At every step, a microscope was used to check the effectiveness of the polishing. Samples were finally polished down to 0.1 μm in the following four different ways and comparative studies were done to select the most efficient one:

1. An auto-polisher was used with diamond suspensions in water of gradation 6 μm, 3 μm, 1 μm, and 0.1 μm as polishing liquids on a texmat cloth;

2. Oil-based diamond suspensions of gradation 6 μm, 3 μm, 1 μm, and 0.1 μm were used to polish samples on a texmat cloth in the auto-polisher;

3. Instead of an auto-polisher, a dimpler was used with diamond suspensions in oil of gradation 3 μm, 1 μm, and 0.1 μm as polishing liquids; and

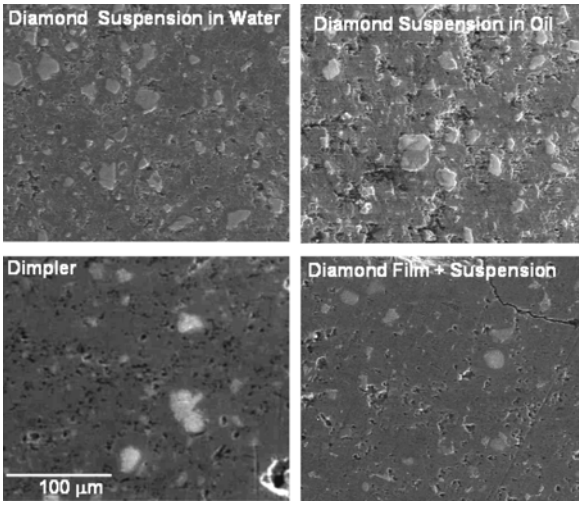


*Fig. 1—Scanning electron microscope image of cement paste samples following different polishing techniques.*

4. Diamond lapping films of gradation 6 μm and 3 μm were used to polish samples down to 3 μm and, as a final step, a diamond suspension in water of 0.1 μm was used in an auto-polisher.

Figure 1 shows SEM images of samples polished using the techniques mentioned previously. After a careful study, it was found that the use of silicon carbide papers down to 6.5 μm, then the use of diamond lapping films of gradation 6 and 3 μm, and finally the use of a diamond suspension in water of 0.1 μm (Method 4) produced a very smooth surface with minimal damage. It was decided not to use a suspension in oil because oil made the samples difficult to clean. Also, a suspension in water did not cause any additional damage compared with a suspension in oil. Instead of using a conventional polishing wheel or an auto-polisher, the effect of using diamond suspension in a dimpler was also investigated. A dimpler is generally used to prepare transmission electron microscopy samples because it applies less force on the sample and offers more controlled polishing. The area polished, however, is relatively small and it is also difficult to polish the exact same area in successive polishing steps. Considering all these, Method 4, as described previously, was selected for the rest of the experiments. For most of the polishing steps, water was avoided. Otherwise, effects, if there were any, due to the use of water were always tested with methods without any water. For longer storage, samples were placed in nitrogen to avoid any change in the microstructure due to atmospheric conditions. As a final step, 0.08 in. (2 mm) thick polished samples were ultrasonically cleaned to remove polishing debris. Both ethanol and water were considered as cleaning medium. Samples cleaned in water for 1 minute did not show any damage compared with samples cleaned in ethanol. Cleaning in water for more than 3 minutes caused sample damage. Considering this, it was decided to clean samples in water for 1 minute for the rest of the experiments.

## IMAGING OF HARDENED CEMENT PASTE

### Experimental details

A scanning probe microscope was used in this study, both in contact and tapping modes, although tapping mode was found to be more effective. Along with AFM, a microscope and an environmental scanning electron microscope were used to find representative areas of the sample after polishing and to

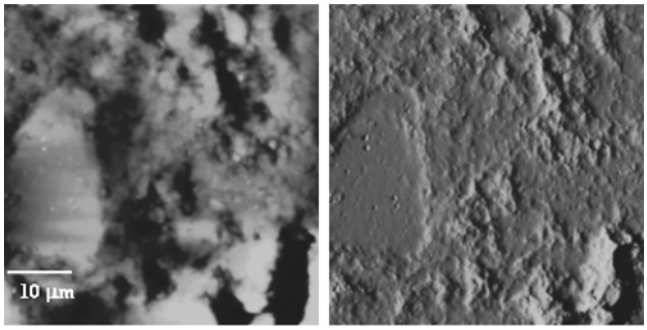


*Fig. 2—50 x 50 μm atomic force microscopy image of polished cement paste: (a) topography; and (b) change in amplitude.*

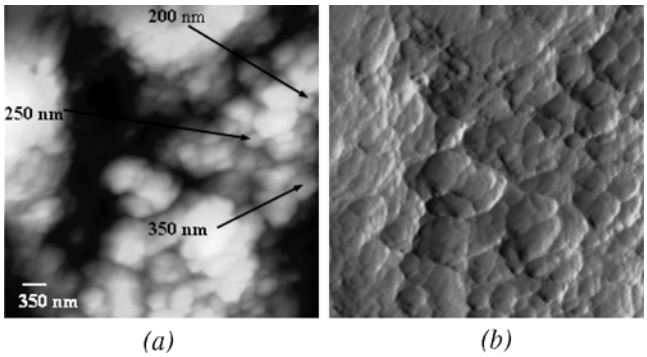


*Fig. 3—4.7 x 4.7 μm AFM image of C-S-H gel: (a) topography; and (b) change in amplitude.*

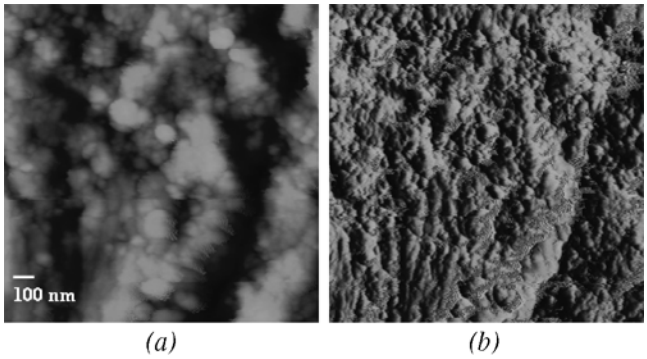


*Fig. 4—1.5 x 1.5 μm atomic force microscopy image of polished cement paste: (a) topography, and (b) change in amplitude.*

provide surface information at millimeter to nanometer scale. SEM was used in low-vacuum mode. AFM images of samples were compared before and after SEM imaging. This was to make sure that the AFM images were not affected by any possible damage that the low-vacuum of the SEM may cause to the samples.

### Results

Figure 2 shows a 50 x 50 μm AFM image of cement paste—on the left, the topography, and on the right, the amplitude signal. The topography image shows the coarse height variations of the sample, brighter regions being higher than darker ones. The amplitude image shows local variations in height after removal of the coarse topography variations, in effect a high-pass filtered image. Because of the large difference in mechanical properties of unhydrated particles and the surrounding cement paste, great care had to be taken to polish both of these phases together with the same effectiveness. The maximum height difference between different areas in this image is 1.5 μm.

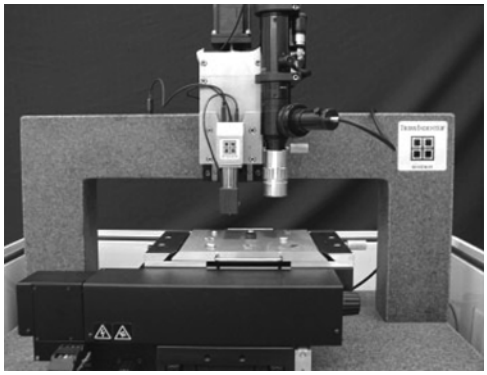

*Fig. 5—Triboindenter.*

Images of C-S-H gel show nearly spherical particles of different sizes in different areas. Depending on the effectiveness of polishing technique, it was possible to image C-S-H particles of different sizes. The sizes of the spherical particles range from 40 nm to 200 to 700 nm. Figure 3 is a 4.7 x 4.7 μm AFM image of C-S-H gel. This clearly shows particles of sizes of 200 to 350 nm. With the most effective polishing technique, it was possible to explore the structure of C-S-H gel at a scale of 40 to 50 nm. Figure 4 is a 1.5 x 1.5 μm AFM image that shows spherical particles of size in the range of 40 nm. It should be noted that the feature size in an AFM image of a somewhat rough material such as this should only be interpreted as an upper bound on the true feature size in the object; in many cases, the images are a convolution of the tip shape and the sample roughness.

## DETERMINATION OF LOCAL MECHANICAL PROPERTIES

### Experimental details

A triboindenter as shown in Fig. 5[33] was used to determine the nano-mechanical properties. Both a Berkovich tip with total included angle of 142.3 degrees and a cube corner tip with total included angle of 90 degrees were used for indentation and SPM imaging. From initial tests, the cube corner tip was found to be more effective for high-resolution imaging because of the smaller included angle and the smaller effective radius (as mentioned previously, there can be an effect due to convolution of the images by the tip radius). The imaging feature using the same indenter tip provides the capability to identify different phases and to position the indenter probe within 10 nanometers of the desired test location. Post-test imaging also provides the ability to verify that the test was performed in the anticipated location, which maximizes the reliability of the data. Multiple cycles of partial loading and unloading were used to make each indent, eliminating creep and size effects.[14] The Oliver and Pharr method was used to determine the mechanical properties[15] where indentation modulus is calculated from the final unloading curve and hardness is defined as the maximum indentation load divided by the contact area.

With the development of more effective polishing techniques as described in the "Sample preparation" section (Method 4), it was found that the Berkovich tip was also capable of

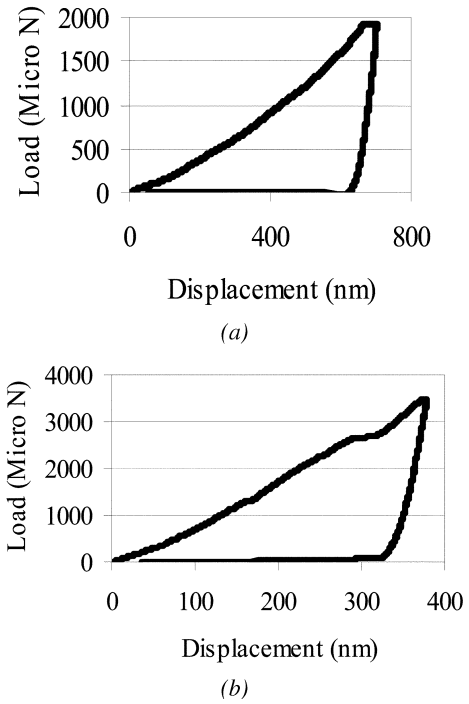


*Fig. 6—Force-displacement plot: (a) acceptable; and (b) possible fracture of material, not acceptable.*

imaging the sample with adequate resolution. This has one advantage over using a cube corner tip because the Oliver and Pharr method gives a slightly higher modulus for most of the materials when a cube corner tip is used. Image of a representative area of a cement paste sample was first captured with the Berkovich tip, and then nearly 60 locations were selected for indentation both on the unhydrated particle and on the area around it. Using the same tip, an image was captured after indentation to make sure that the indents were made at the desired locations. This whole testing process was repeated on 10 different areas of three different samples. Some of the indentation test data were discarded due to the irregular nature of the load-displacement plot (Fig. 6), which could be due to the presence of a large void or cracking of the material.

## Results

Figure 7 shows images of different areas after indentation, and Fig. 8 shows that the elastic modulus decreases with distance from an unhydrated particle. For unhydrated particles, the calculated modulus and the hardness values were 125 and 7.66 GPa (18,130 and 1111 ksi), respectively. For C-S-H gel close to an unhydrated particle, the values measured were 40 and 1.32 GPa (5802 and 191 ksi). For C-S-H gel further away from an unhydrated particle, the calculated modulus was 23 GPa (3336 ksi) and the hardness 1.01 GPa (146 ksi). Difference in mechanical properties of the C-S-H gel in different areas was repeatedly observed.

Figure 9 shows a 60 x 60 μm image of a cement paste with a bright, unhydrated particle near the center. It also shows the modulus values calculated from the indentation data. Values are written on the respective indent locations on the image. Again, observed mechanical properties of the C-S-H gel in different areas were different. Statistical analysis showed that a normal distribution can be fitted for the variation in modulus with a mean of 19 GPa (2756 ksi) and standard

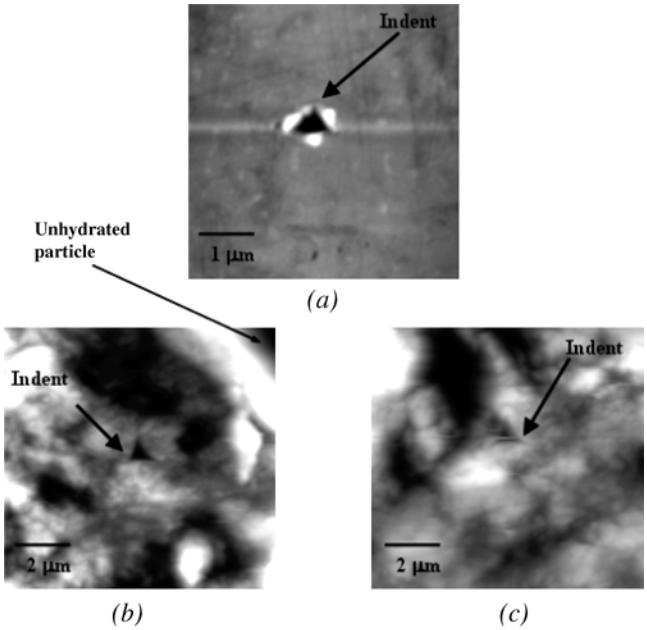


*Fig. 7—(a) 5 x 5 μm image of unhydrated particle after indentation; (b) 10 x 10 μm image of C-S-H gel close to unhydrated particle; and (c) 10 x 10 μm image of C-S-H gel further away from unhydrated particle.*

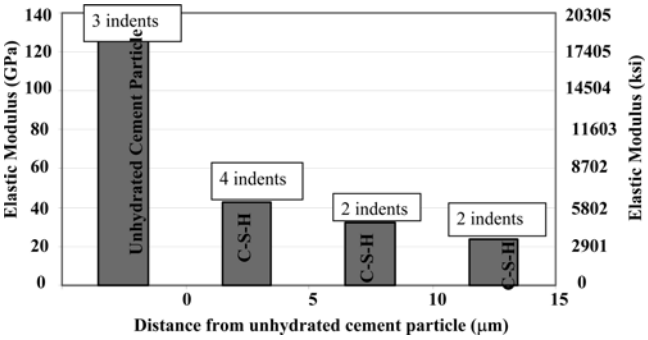


*Fig. 8—Change in modulus of C-S-H with distance from unhydrated particle.*

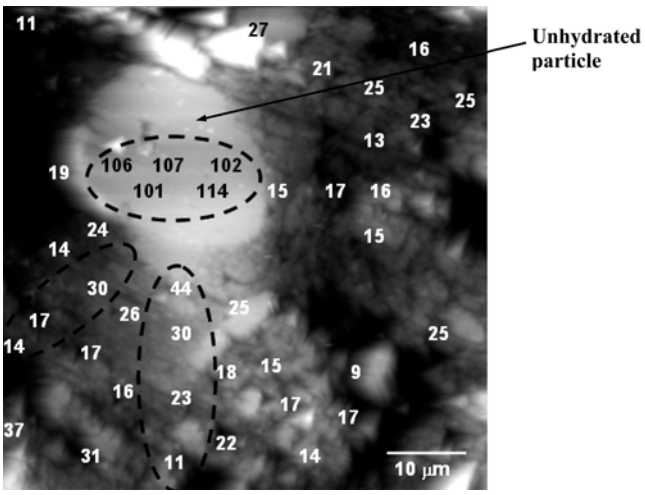


*Fig. 9—60 x 60 μm image of gel with unhydrated particle showing locations of indents and Young's modulus in GPa.*

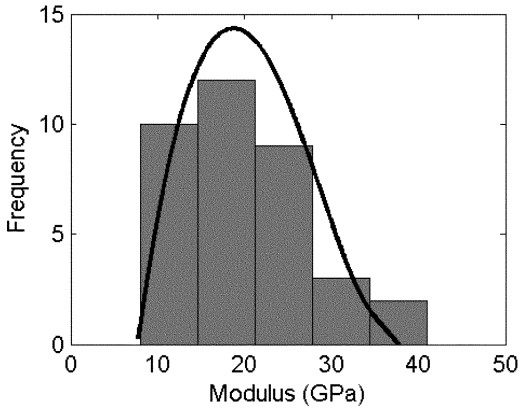


*Fig. 10—Frequency plot of calculated Young's modulus with fitted normal distribution.*

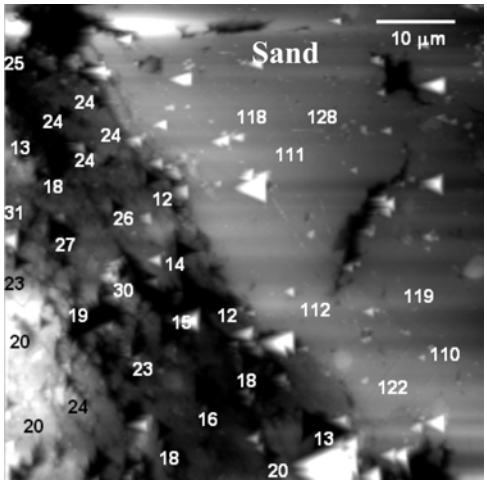


*Fig. 11—60 x 60 μm image of gel with sand particle and ITZ showing locations of indents and Young's modulus in GPa.*

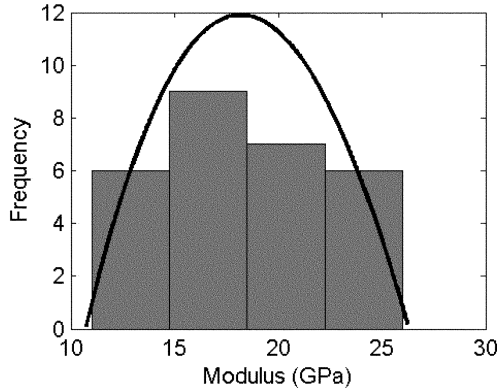


*Fig. 12—Frequency plot of calculated Young's modulus in ITZ with fitted normal distribution.*

deviation of 7.2 GPa (1044 ksi). Figure 10 shows the frequency distribution plot of the data. Effect of bin size on the frequency distribution plot was investigated and a frequency plot with smaller bin size showed two high peaks, one in the range of 20 to 25 GPa (2900 to 3626 ksi) and another one in the range of 30 to 35 GPa (4351 to 5076 ksi). This correlates well with the mean of the bimodal distribution of the modulus reported by Constantinides and Ulm[16] and Constantinides et al.,[17] though the data did not represent a combination of two normal distributions. The Young's moduli of unhydrated particles as obtained in this study are a little lower than the results reported by Velez et al.[18] This is expected because Velez et al. used pure clinker phases, whereas unhydrated cement particles seem to be more porous. As seen in the initial study, many areas show a decreasing trend in the modulus values with the distance from the unhydrated cement particles. From a more rigorous test like this one, however, it is clear that there are low stiffness areas near the unhydrated particles, as can be shown in Fig. 9. Similar tests have been repeated on different samples ten times and the results are reproducible. On an area without an unhydrated cement particle nearby, modulus values obtained are in a range of 25 to 15 GPa (3626 to 2176 ksi), which is less than values observed around unhydrated cement particles.

**Table 1—Average Young's modulus of different phases of cement paste and mortar**

| | Unhydrated cement particle | Cement paste matrix | Interfacial transition zone |
|---|---|---|---|
| Average Young's modulus, GPa (ksi) | 110 (15,954) | 21 (3046) | 18 (2611) |

Note: 1 GPa = 145.038 ksi.

## DETERMINATION OF LOCAL MECHANICAL PROPERTIES OF ITZ

### Experimental details

Cement paste samples were cast with Illinois river sand particles in them. These are model mortar samples with few sand particles to create ITZ. To avoid complexity, sand particles with size between 1.18 and 2.36 mm (0.05 to 0.09 in.) were used. These were cured and polished following the same procedure as described for cement paste samples. Because of the large difference in mechanical properties between the sand particle and the ITZ, great care had to be taken to have a smooth ITZ to do the nanoindentation tests. Sand particles being much stiffer than the ITZ, they have a tendency to stick out of the sample, which makes imaging and indentation difficult at the extreme vicinity of the particle. After careful sample preparation, nanoindentation tests were performed, imaging the area before and after indentation to ensure the effectiveness of the sample preparation, representativeness of the area under investigation, and finally to make sure that the indentations were done at the desired locations.

### Results

Figure 11 shows an image of the ITZ with a sand particle on the right side. Imaging along with nanoindentation proved to be the most effective in identifying the narrow area of ITZ and in performing nanoindentation on the same region. After imaging, approximately 50 locations were chosen on the sand particle and on the cement paste. Superimposed on the image are the Young's modulus values obtained from the nanoindentation tests. The Young's modulus is clearly less near the sand particle and increases with distance. There are areas near the sand particle that seem stronger and less porous from the image, and these show a higher modulus as would be expected—for instance, the area near the top left-hand corner of the image. For this particular test set, similar statistical analysis showed that a normal distribution can be fitted for the variation in modulus with a mean of 18 GPa (2611 ksi) and standard deviation of 4.3 GPa (624 ksi). Figure 12 shows the frequency distribution plot of the data.

Results presented herein compare well with the results of Zhu and Bartos[30] and Zhu et al.[31] Considering all the test data in different regions, Table 1 presents the average Young's modulus for unhydrated cement particles, paste matrix, and interfacial transition zone where the average modulus of ITZ is 85% of that of the paste matrix. This compares well with the modeling results of Sun et al.[28]

## CONCLUSIONS

From this study, it has been found that AFM is a promising technique to image and characterize cement paste micro- and nano-structure. The structure of C-S-H gel in different areas showed spherical particles of different sizes in the range of 40 nm to 200 to 700 nm. It has also been found that sample preparation is very critical for micro- or nano-scale characterization. With the development of an improved polishing protocol, it was found that in many areas of C-S-H, there were spherical particles as small as 40 nm.

This study also shows that nanoindentation along with imaging is a powerful technique to determine the mechanical properties of different phases of cement paste micro- and nano-structure. The Young's modulus of unhydrated cement particles and C-S-H gel has been determined, and differences in the Young's modulus have been found in different areas of cement paste microstructure. In many cases, paste around unhydrated particles has a higher modulus. Using the imaging capability of the nanoindenter tip, it was possible to position the indenter exactly in the narrow region of ITZ and perform nanoindentation to determine the local mechanical properties directly. It was found that the paste in the ITZ has, in general, a lower Young's modulus.

## ACKNOWLEDGMENTS

This research was performed as part of Federal Highway Administration Grant (Award No. DTFH61-05-C-0001).

## REFERENCES

1. Binnig, G.; Quate, C. F.; and Gerber, C., "Atomic Force Microscope," *Physical Review Letters*, V. 56, No. 9, Mar. 1986.

2. Mitchell, L. D.; Prica, M.; and Birchall, J. D., "Aspects of Portland Cement Hydration Studied Using Atomic Force Microscopy," *Journal of Materials Science*, V. 31, 1996, pp. 4207-4212.

3. Yang, T.; Keller, B.; and Magyari, E., "AFM Investigation of Cement Paste in Humid Air at Different Relative Humidities," *Journal of Physics D: Applied Physics*, V. 35, 2002, pp. L25-L28.

4. Yang, T.; Keller, B.; Magyari, E.; Hametner, K.; and Günther, D., "Direct Observation of the Carbonation Process on the Surface of Calcium Hydroxide Crystal in Hardened Cement Paste Using Atomic Force Microscope," *Journal of Materials Science*, V. 38, 2003, pp. 1909-1916.

5. Papadakis, V. G.; Pedersen, E. J.; and Lindgreen, H., "An AFM-SEM Investigation of the Effect of Silica Fume and Fly Ash on Cement Paste Microstructure," *Journal of Materials Science*, V. 34, 1999, pp. 683-690.

6. Kauppi, A.; Andersson, K. M.; and Bergström, L., "Probing the Effect of Superplasticizer Adsorption on the Surface Forces Using the Colloidal Probe AFM Technique," *Cement and Concrete Research*, V. 35, 2005, pp. 133-140.

7. Nonat, A., "The Structure and Stoichiometry of C-S-H," *Cement and Concrete Research*, V. 34, 2004, pp. 1521-1528.

8. Plassard, C.; Lesniewska, E.; Pochard, I.; and Nonat, A., "Investigation of the Surface Structure and Elastic Properties of Calcium Silicate Hydrates at the Nanoscale," *Ultramicroscopy*, V. 100, Issues 3-4, Aug. 2004, pp. 331-338.

9. Reynaud, C.; Summer, F.; Que, C.; El Bounia, C.; and Duc, T. M., "Quantitative Determination of Young's Modulus on a Biphase Polymer System Using Atomic Force Microscopy," *Surface and Interface Analysis*, V. 30, 2000, pp. 185-189.

10. Bischel, M. S.; Vanlandingham, M. R.; Eduljee, R. F.; Gillespie, J. W. Jr.; and Schultz, J. M., "On the Use of Nanoscale Indentation with the AFM in the Identification of Phases in Blends of Linear Low Density Polyethylene and High Density Polyethylene," *Journal of Materials Science*, V. 35, No. 1, Jan. 2000, pp. 221-228.

11. Vanlandingham, M. R.; McKnight, S. H.; Palmese, G. R.; Eduljee, R. F.; Gillespie, J. W. Jr.; and McCulough, R. L., "Relating Elastic Modulus to Indentation Response using Atomic Force Microscopy," *Journal of Materials Science Letters*, V. 16, No. 2, Jan. 1997, pp. 117-119.

12. Fischer-Cripps, A. C., *Nanoindentation*, 2nd Edition, Springer-Verlag, New York, 2004, 266 pp.

13. Hughes, J. J., and Trtik, P., "Micro-Mechanical Properties of Cement Paste Measured by Depth-Sensing Nanoindentation: A Preliminary Correlation of Physical Properties with Phase Type," *Materials Characterization*, V. 53, Issues 2-4, Nov. 2004, pp. 223-231.

14. Nemecek, J.; Kopecky, L.; and Bittnar, Z., "Size Effect in Nanoindentation of Cement Paste," *Proceedings of the International Conference*, University of Dundee, Scotland, UK, July 2005, pp. 47-53.

15. Oliver, W. C., and Pharr, G. M., "An Improved Technique for Determining Hardness and Elastic Modulus using Load and Displacement Sensing Indentation Experiments," *Journal of Material Research*, V. 7, 1992, pp. 1564-1583.

16. Constantinides, G., and Ulm, F. J., "The Effect of Two Types of C-S-H on the Elasticity of Cement-Based Materials: Results from Nanoindentation and Micromechanical Modeling," *Cement and Concrete Research*, V. 34, 2004, pp. 67-80.

17. Constantinides, G.; Ulm, F. J., and Van Vliet, K., "On the Use of Nanoindentation for Cementitious Materials," *Materials and Structures/ Materiaux et Constructions*, V. 36, No. 257, Apr. 2003, pp. 191-196.

18. Velez, K.; Maximilien, S.; Damidot, D.; Fantozzi, G.; and Sorrentino, F., "Determination by Nanoindentation of Elastic Modulus and Hardness of Pure Constituents of Portland Cement Clinker," *Cement and Concrete Research*, V. 31, 2001, pp. 555-561.

19. Ebenstein, D. M., and Wahl, K. J., "Anisotropic Nanomechanical Properties of Nephila Clavipes Dragline Silk," *Journal of Materials Research*, V. 21, No. 8, 2006, pp. 2035-2044.

20. Bentz, D. P; Schlangen, E.; and Garboczi, E. J., "Computer Simulation of Interfacial Zone Microstructure and its Effect on the Properties of Cement-Based Composites," *Materials Science and Concrete IV*, J. P. Skalny and S. Mindell, eds., American Ceramic Society, Westerville, OH, 1995, pp. 155-199.

21. Scrivener, K. L.; Crumbie, A. K.; and Laugesen P., "The Interfacial Transition Zone (ITZ) between Cement Paste and Aggregate in Concrete," *Interface Science*, V. 12, 2004, pp. 411-421.

22. Simeonov, P., and Ahmad, S., "Effect of Transition Zone on the Elastic Behavior of Cement-Based Composites," *Cement and Concrete Research*, V. 25, No. 1, 1995, pp. 165-176.

23. Hu, J.; and Stroeven, P., "Properties of the Interfacial Transition Zone in the Model Concrete," *Interface Science*, V. 12, 2004, pp. 389-397.

24. Li, G.; Zhao, Y.; and Pang, S., "Four-Phase Sphere Modeling of Effective Bulk Modulus of Concrete," *Cement and Concrete Research*, V. 29, 1999, pp. 839-845.

25. Li, G.; Zhao, Y.; Pang, S. S.; and Li, Y., "Effective Young's Modulus Estimation of Concrete," *Cement and Concrete Research*, V. 29, 1999, pp. 1455-1462.

26. Lutz, M. P.; Monteiro, P. J. M.; and Zimmerman, R. W., "Inhomogeneous Interfacial Transition Zone Model for the Bulk Modulus of Mortar," *Cement and Concrete Research*, V. 27, No. 7, 1997, pp. 1113-1122.

27. Nadeau, J. C., "Water-Cement Gradients in Mortars and Corresponding Effective Elastic Properties," *Cement and Concrete Research*, V. 32, 2001, pp. 481-490.

28. Sun, Z.; Garboczi, E. J.; and Shah, S. P., "Modeling the Elastic Properties of Concrete Composites: Experiment, Differential Effective Medium Theory, and Numerical Simulation," *Cement & Concrete Composites*, V. 29, 2007, pp. 22-38.

29. Ramesh, G.; Sotelino, E. D.; and Chen, W. F., "Effect of Transition Zone on Elastic Moduli of Concrete Materials," *Cement and Concrete Research*, V. 26, 1996, pp. 611-622.

30. Zhu, W., and Bartos, P. J. M., "Application of Depth-Sensing Microindentation Testing to Study of Interfacial Transition Zone in Reinforced Concrete," *Cement and Concrete Research*, V. 30, 2000, pp. 1299-1304.

31. Zhu, W.; Sonebi, M.; and Bartos, P. J. M., "Bond and Interfacial Properties of Reinforcement in Self-Compacting Concrete," *Materials and Structures/Materiaux et Constructions*, V. 37, Aug.-Sept. 2004, pp. 442-448.

32. Asbridge, A. H.; Page, C. L.; and Page, M. M., "Effects of Metakaolin, Water/Binder Ratio and Interfacial Transition Zones on the Microhardness of Cement Mortars," *Cement and Concrete Research*, V. 32, 2002, pp. 1365-1369.

33. *Triboindenter User Manual*, Hysitron Inc., Minneapolis, MN.